

# **Valorisation of water treatment sludge for lightweight aggregate production**

J. Mañosa<sup>a</sup>, J. Formosa<sup>a</sup>, J. Giro-Paloma<sup>a</sup>, A. Maldonado-Alameda<sup>a</sup>, M.J. Quina<sup>b</sup>, J.M. Chimenos<sup>a,\*</sup>

<sup>a</sup>Departament de Ciència de Materials i Química Física, Universitat de Barcelona, C/ Martí i Franquès 1, 08028, Barcelona, Spain.

<sup>b</sup>CIEPQPF- Chemical Process Engineering and Forest Products Research Centre, Department of Chemical Engineering, University of Coimbra, Rua Sílvio Lima, Coimbra, 3030-790, Portugal

\* Corresponding author e-mail: [chimenos@ub.edu](mailto:chimenos@ub.edu)

## **Abstract**

Water treatment sludge is an industrial by-product which has recently been classified as a waste by the European Commission. The main goal of this work is to valorise this waste to produce lightweight aggregates. Formulations with sludge substituting expanded clay up to 50 wt.% were produced. The physical properties of the lightweight aggregates such as bloating index, density and porosity were studied. The introduction of the sludge without expanding properties, reduced the expandability of the clay and the porosity of the aggregates. The density increased from 0.32 g/cm<sup>3</sup> in aggregates without sludge to 1.46 g/cm<sup>3</sup> in aggregates with 50 wt.% of sludge. It is shown that lightweight aggregates can be produced using mixtures of expanded clay and water treatment sludge, with low substitution percentages (up to 15 wt.% of sludge). Aggregates up to 15 wt.% of sludge were further studied. The compressive strength increased with sludge wt.%, and the concentrations of heavy metals and metalloids, assessed through leaching tests, were well below the established limits. Two preliminary tests of lightweight aggregate concrete were produced: LWAC 1 was formulated with commercial lightweight aggregates and LWAC 2 with aggregates containing 7 wt.% of the sludge and commercial lightweight aggregates. The physical, mechanical and thermal properties of LWAC 1 and LWAC 2 were found to be very similar. Our work demonstrates the feasibility in using water treatment sludge as a by-product to produce lightweight aggregates suitable for thermal insulation and lightweight applications.

*Keywords:* Lightweight aggregate; water treatment sludge; expanded clay; lightweight aggregate concrete; waste valorisation.

## 1. Introduction

The increase in waste generated in Europe represents a concern for modern society. This increase is mainly due to the growth of population and to the urbanization. As a solution, the Waste Framework Directive (2008/98/EC) is promoting the research of viable alternatives for managing waste. In this sense, the studies must include new findings regarding the residues reuse from different sources, by formulating them into secondary materials [1]. On the other hand, social development requires increased production of drinking water. Henceforth, to acquire potable water, surface water requires proper treatment which is performed in water treatment plants (WTPs) [2]. The processes involved in water treatment are mainly coagulation-flocculation, sedimentation, filtration and disinfection [3]. During the water treatment process, the water treatment sludge (WTS) residue is generated to remove the impurities of the raw water. An increment of WTS will occur with the expected increase in drinking water demand [4]. Most of WTS is originated in the coagulation-flocculation process, and its composition highly depends on the coagulants' chemical nature (and flocculants) used in the water treatment. One of the most common coagulants is poly-aluminium chloride (PACl). When PACl is added into the water, dissolved aluminium ions ( $\text{Al}^{3+}$ ) and precipitates of aluminium hydroxides ( $\text{Al}(\text{OH})_3$ ) help to aggregate particles contained in raw water into larger flocs [5]. These flocs of  $\text{Al}(\text{OH})_3$  constitute the major portion of WTS, together with silt, clay, sand, other particles removed from raw water, and other chemical products used in the water treatment. Therefore, although there is a small organic content, WTS is mostly inorganic, and the composition of the sludge strongly depends on the raw water source [6,7].

A model WTP produces around 100,000 t of sludge every year [2]. Recently, several countries have restricted the WTS disposal because WTS has been classified as waste from Commission Decision 2014/955/EU (amendment of Commission Decision 2000/532/EC). Therefore, WTS must be disposed of properly in landfills [8], while more eco-friendly solutions are found. Indeed, WTS has been reused to formulate materials taking advantage of its similar composition (mainly inorganic) to clay and shale.

In particular, applications in ceramic and construction sectors have been studied, such as in the production of bricks, tiles, clinker and alternative cements (alkali-activated cements) [8–13]. Moreover, applications in chemical processes and as a coagulant in wastewater treatment were also tested [7,14].

In order to avoid the exhaustion of resources in the construction industry, waste could partially replace raw materials, leading to a circular economy approach. Moreover, some waste can be recovered as useful materials to preserve natural resources, such as the recovery of ore-body pillars from mining underground [15]. These possibilities have prompted the emergence of new research lines aimed at developing sustainable materials and valorising residues. A noticeable example is the development of aggregates, mainly for concrete and mortar formulations. In 2015, approximately 48,300 Mt of aggregates were produced to fulfil the construction industry demand [16]. Among these aggregates, those with very low particle density (up to  $2 \text{ g/cm}^3$ ) are known as lightweight aggregates (LWA) [17]. LWA are granulated materials mainly obtained by a) directly from natural resources, like pumice, perlite, volcanic scoria, and ashes [18,19], or b) manufactured by firing in a kiln raw materials with expansive properties like vermiculite, shale or clay at temperatures from  $1,000 \text{ }^\circ\text{C}$  to  $1,300 \text{ }^\circ\text{C}$  (rapid sintering) [1,20,21]. LWA are used to formulate a broad range of products such as lightweight aggregate concrete (LWAC), lightweight geotechnical fills, and insulation products, among others. LWA can be used in a number of applications such as soil engineering, hydroculture, drainage, roof gardens, and filters [1], where LWAC is the application which requires larger volumes of LWA. The addition of LWA to cement to produce LWAC, improves the thermal insulation of buildings, which results in an increase of its energy efficiency [22,23]. The reduction in the total weight of the concrete when incorporating LWA, is useful for applications such as lightweight floors and walls, facades and signs [24,25]. The construction sector is responsible for around 40 % of global energy consumption and 30 % of total greenhouse gas emissions [26], and the production of LWAC with waste-based LWA would benefit both sustainability and energy efficiency in buildings.

Expanded manufactured LWA to be used in concretes should have a highly porous internal structure and an impermeable external surface [27]. Two conditions are necessary to obtain expanded LWA by the rapid sintering process: the presence of substances that release gases during the thermal treatment, and the existence of a glassy phase to trap these gases [1,28,29]. Specifically, a substance that creates a highly viscous phase during the firing process is needed to entrap gases, thus generating a porous structure during the bloating process. The viscosity of this phase is strictly given by the raw material composition and can be expressed in a ternary diagram known as bloating diagram [29]. The gases that cause the expansion phenomena may arise from thermal decomposition of specific constituents. These decompositions can be water vaporization from the interlayer water molecules or crystallization water, CO and CO<sub>2</sub> generation from organic matter and carbonates, among others [28,30]. LWA have the potential of using waste as raw material for its formulation, by partially replacing clay [17]. For that purpose, waste that release a high volume of gas when heated are interesting materials, as they can help to create the required porous structure [1,31]. Some of the residues used as raw materials in LWA production are fly-ash, sewage sludge, waste glass, sugarcane and municipal solid waste incineration bottom ash among others [32–35]. The observed high thermal weight loss in WTS suggests that WTS can be suitable to replace raw materials to produce LWA, while still keeping the desired properties [36–38].

The aim of this work is to evaluate the possibility of substituting expanded clay for WTS in the production of LWA. The sustainability of LWA would increase by reusing a waste, and WTS would have the added value of avoiding landfilling. To that aim we have produced LWA with different clay-WTS formulations and we have performed an exhaustive characterisation of their properties. Furthermore, the behaviour of the LWA in concrete has been assessed by comparing two preliminary tests of LWAC: a LWAC prepared with commercial LWA and another one prepared with LWA produced in this work.

## 2. Materials and methods

### 2.1. Materials

A sample of WTS was collected from a WTP (Ens d'Abastament d'Aigua Ter-Llobregat, ATL) located in Cardedeu (Barcelona, Spain). The sample of WTS was randomly selected from the sludge stockpiled in the water potabilization plant and lately quartered to obtain a representative sample, following the standard EN 14899 [39]. The plant supplies drinking water coming from raw water from the Ter river. The plant has a maximum water treatment capacity of 8 m<sup>3</sup>/s. WTS is produced during a conventional water treatment process and centrifuged before its disposal. Approximately 50 t of centrifuged WTS are generated in this WTP per day. The natural clay used in this project was provided by a Portuguese industrial plant, which processes about 24 t/h of clay to produce commercial LWA. Both raw materials were mixed to develop handcrafted LWA formulated as shown in Table 1. Besides, commercial LWA of three different sizes (small (S, 1-5 mm), medium (M, 4-12.5 mm) and large (L, 10-20 mm)) provided by Leca International Company as well as selected LWA synthesized in the laboratory were used to obtain two LWAC samples. For both LWAC, the binder used was ordinary Portland cement (OPC) CEM I 52.5 R from Cementos Molins, a typical cement to produce precast, which could be one of the main applications of the LWAC. The properties of the OPC and LWA used to produce LWAC can be found in supplementary material in Tables S1 and S2 respectively.

Table 1.- Formulation of unfired spherical pellets.

Reference	Clay (wt.%)	WTS (wt.%)	Water (wt.%)	Mineral Oil (wt.%)
0 wt.% WTS	100	0	30	1
2 wt.% WTS	98	2	30	1
5 wt.% WTS	95	5	30	1
7 wt.% WTS	93	7	30	1
10 wt.% WTS	90	10	30	1
13 wt.% WTS	87	13	30	1
15 wt.% WTS	85	15	30	1
20 wt.% WTS	80	20	30	1
50 wt.% WTS	50	50	30	1

## 2.2. Experimental procedure

### 2.2.1. *Production of LWA*

The limit region of Riley's Ternary diagram, indicated with a dashed line in Fig. 1, is a delimited zone of compositions ( $\text{SiO}_2 - \text{Al}_2\text{O}_3 - \text{Fluxing oxides}$ ). This region gives a range of compositions of clay-like materials that present expansive properties when fired [29]. The possibility to produce LWA only from WTS was studied elsewhere with promising results [36]. As the sludge from this work is outside of the dashed line, the WTS did not bloat by means of rapid sintering. Therefore, as the WTS used in this study did not have the composition required to produce LWA, the WTS was tested for the replacement of different percentages of clay up to 50 wt.% (see Table 1). The formulations from 0 to 15 wt.% of WTS were chosen with small intervals between them since the low substitution formulations were the most promising ones, as their compositions plotted in the ternary diagram were found inside the bloating area. The addition of 20 wt.% of WTS was chosen in order to study the behaviour of aggregates produced with a composition in the limit of the bloating area, while the 50 wt.% of WTS formulation was chosen to evaluate the expansion of aggregates with a composition outside of the bloating area.

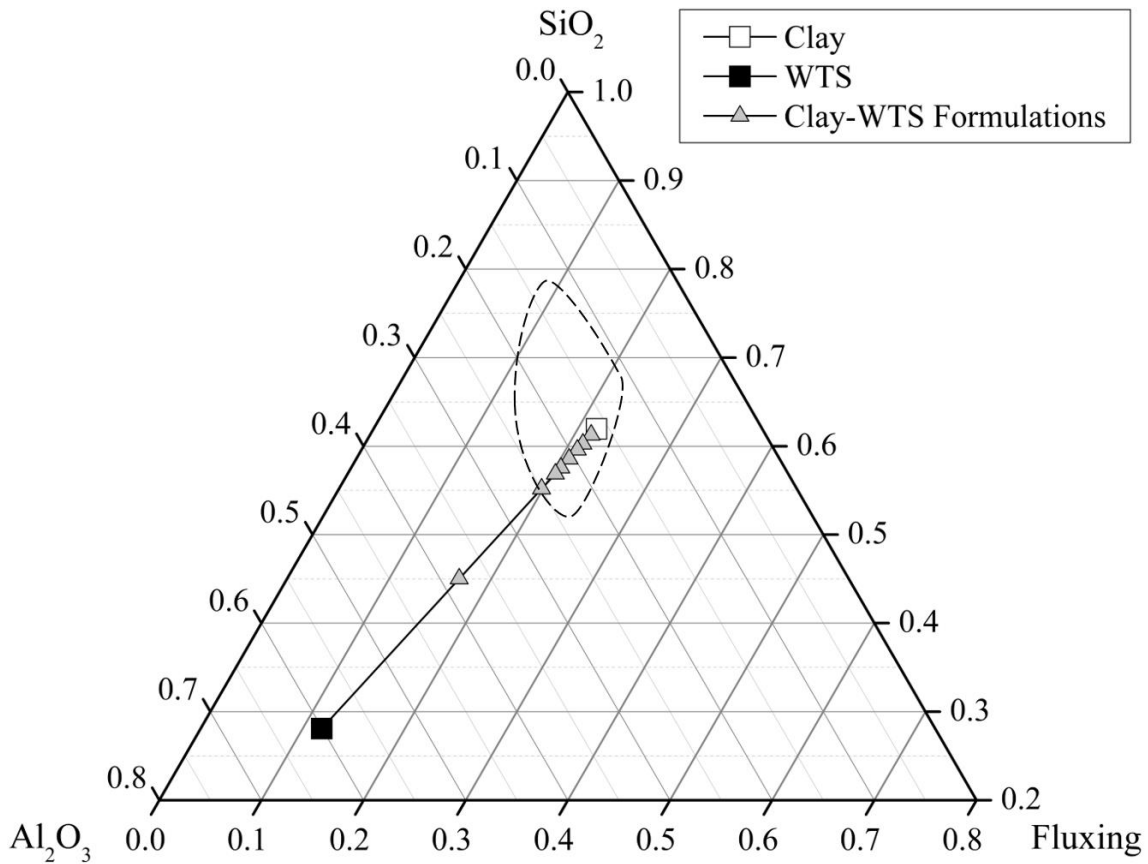


Fig. 1.- Composition of clay, WTS, clay-WTS formulations and bloating area (dashed line).

Clay and WTS were dried at 105 °C during 24 h, ground in a ball mill and sieved (through a 80 µm sieve) to obtain fine and homogeneous powder, suitable for producing unfired spherical (ball-shaped) pellets. In addition, deionised water and commercial mineral oil were used in the pellets preparation, mimicking the industrial recipe. The process to prepare the raw materials and the LWA formulations is described in a previous study [1]. Initially, both raw materials were mixed according to the proportions in Table 1 and the mixture was homogenized. Deionised water (~ 30 wt.%) and mineral oil (~1 wt.%) were added to the homogenized powder mixture to obtain proper consistency, workability, and plasticity. These properties are important to give the desired shape to the mixture, and to obtain unfired pellets without cracks (due to lack of water) or unable to maintain its shape (due to an excess of water). Handcrafted spherical unfired pellets were obtained. Subsequently, the unfired pellets were dried at 105 °C for 24 h, pre-heated, and finally fired in a muffle furnace. The fired pellets were quenched in air to get the glassy external shell that will trap the gases, thus resulting in the



required porous internal structure. The pre-heating stage was set at 200 °C for at least 2 h to simulate the industrial process of LWA production in a rotatory kiln [21,40]. The optimal firing temperature and time (1,175 °C for 8 min) were determined through dilatometry and preliminary rapid sintering tests of unfired pellets formulated only with clay.

### 2.2.2. LWAC formulation

To evaluate the effect of LWA in concrete, two preliminary LWAC formulations were prepared: one of them with commercial LWA (LWAC 1), and another one with the LWA prepared and selected from this study (LWAC 2). The gradation of all the aggregates was evaluated. Commercial fired aggregates of S, M and L sizes, and LWA prepared in this project with 7 wt.% of WTS were used (the properties of all LWA are presented in the supplementary material, Table S2). Gradation, theoretical Fuller gradation (both in mass % passing) and fineness modulus (FM) of the aggregates are compiled in Table 2. A low value of FM indicates fine aggregates and high value of FM indicates coarse aggregates. All the LWA gradations were almost uniform, which means that the aggregates are almost single sized [41]. Taking into account that the main purpose of the LWAC developed was to increase thermal insulation, regardless of the technological properties of the concrete, the amount of aggregates was maximised because this maximises the porosity, and the OPC content was minimised. To reach this target, the maximum compactness of the LWA was achieved according to Fuller’s methodology [42,43]. It should be emphasized that only the LWA with particle size > 2 mm were used, and no fine aggregates as sand or crushed LWA were added. In addition, as the gradation of the developed LWA with 7 wt.% of WTS presented lack of small aggregates (see Table 2, high FM), the smaller commercial aggregates with the lowest FM (size S) were added to increase the compactness.

Table 2.- Gradation of LWA to produce LWAC.

Sieve size (mm)	% Passing				
	Commercial LWA			Synthesized LWA	Theoretical distribution
	S	M	L	7 wt.% WTS	Fuller
32	100.00	100.00	100.00	100.00	100.00

<b>16</b>	100.00	100.00	82.63	65.98	70.71
<b>8</b>	100.00	63.82	1.76	17.79	50.00
<b>4</b>	72.90	6.41	0.32	0.20	35.36
<b>2</b>	0.00	0.00	0.00	0.00	25.00
<b>FM</b>	1.27	2.30	3.15	3.16	2.19

S = Small LWA (1-5 mm); M = Medium LWA (4-12.5 mm); L = Large LWA (10-20 mm).

Once the theoretical formulations were calculated, the LWA mixtures were made. The apparent volume of LWA was measured by placing the aggregates in a graduated cylinder and filling it with water. Water filled the voids, and the volume of the voids corresponds to the minimum volume of cement necessary to formulate the dosage proportion for the LWAC development. The required mass of cement was calculated taking into account the cement density obtained from the provider. Generally, LWA from expanded clay exhibit higher water absorption than normal weight aggregates. This absorption causes a reduction in the workability of the fresh concrete [44], and that cement does not have enough water to properly set. To circumvent these problems, LWA are usually saturated in water (pre-wetting) for 24 h before mixing, and then surface dried [44–46]. Several studies pointed to the incorporation of saturated LWA to provide an internal water source to the cement reactions, known as internal curing. This would replace the water consumed during the chemical reactions of the curing process, known as internal curing [47,48]. In our case, the LWA were immersed in water for 24 h to reach the water saturation and LWAC were produced according to the proportions given by Fuller's equations [42]. Aggregates, cement, and water contents are compiled in Table 3. The water content refers to the kneading water and to the water contained in the surface dried LWA. Therefore, water to cement ratio (w/c) is higher than in conventional concrete to reach the desired consistency for proper mould casting. The LWAC specimen sizes were 40 x 150 x 150 mm, as standardized size (40 x 40 x 160 mm) is not large enough to ensure reliable thermal conductivity results. The curing time was 28 days, in a curing room at 20 °C and 95 % of relative humidity.

Table 3.- Mix proportions of LWAC 1 and LWAC 2.

<b>Reference</b>	<b>LWA (kg/m<sup>3</sup>)</b>	<b>kg/m<sup>3</sup></b>	<b>w/c ratio</b>
------------------	-------------------------------	-------------------------	------------------

	S	M	L	7 wt.% WTS	cement	water	
<b>LWAC 1</b>	168	33	156	-	442	320	0.72
<b>LWAC 2</b>	183	-	-	174	440	310	0.70

S = Small LWA (1-5 mm); M = Medium LWA (4-12.5 mm); L= Large LWA (10-20 mm).

### 2.2.3. Characterization

A summary of the assays performed in this study is shown in Table 4. X-ray fluorescence (XRF) semi-quantitative analysis was performed to evaluate the content of most stable oxides in the raw materials, using a Panalytical Philips PW 2400 sequential X-ray spectrometer. The mineral phases were determined by X-ray diffraction (XRD) in a Bragg-Brentano Siemens D-500 powder diffractometer with CuK $\alpha$  radiation with the X'Pert HighScore software. The thermogravimetric analysis (TGA) was accomplished in the raw materials using SDT Q600 device from TA Instruments, in an air atmosphere (50 mL/min) with a heating rate of 10 °C/min up to 1,200 °C. The total organic carbon (TOC) was determined in raw materials with a Thermo EA 1108 (Thermo Scientific), working in standard conditions (helium flow at 120 mL/min, combustion furnace at 1,000 °C, chromatographic column oven at 60 °C, oxygen loop 10 mL at 100 kPa) to complement the determination of thermal decompositions. The specific surface area (SSA) was evaluated using the Brunauer-Emmett-Teller (BET) model with a TriStar 3000 V6.04 A. The particle size distribution (PSD) was measured through a Beckman Coulter<sup>®</sup> LSTM 13 320 device with a universal liquid module. A dilatometry assay was performed to determine the bloating properties, by using an Expert System Solutions S.r.l.-Horizontal Optical Dilatometer Misura<sup>®</sup> with a heating rate of 10 °C/min.

For the synthesized LWA, the weight loss (WL) during the thermal treatment, the bloating index (BI), the apparent density ( $\rho_a$ ), porosity, particle density and water absorption were evaluated. WL, BI and  $\rho_a$  were determined after sizing and weighing the samples. BI was calculated according to Eq. 1,

$$BI (\%) = \frac{V_f - V_i}{V_i} \cdot 100 \quad \text{Eq. 1.}$$

where  $V_i$  and  $V_f$  are the volumes before and after sintering the LWA, respectively. Porosity results are given by image analysis of embedded and cut LWA with the ImageJ software to observe the internal structure. Particle density ( $\rho_{\text{part}}$ ) and water absorption were calculated according to EN 1097-6 standard [49], using Archimedes' principle.

Mechanical properties were tested by means of compressive strength ( $\sigma_c$ ) of the individual sintered LWA, using a Zwick Roell Zmart-PRO machine equipped with a 10 kN load cell, at a loading rate of 2 mm/min. The  $\sigma_c$  was calculated using Eq. 2 [50,51], where  $X$  is the diameter of the spherical LWA (mm) and  $P_c$  the fracture load (N).

$$\sigma_c \text{ (MPa)} = \frac{2.8 \cdot P_c}{\pi \cdot X^2} \quad \text{Eq. 2}$$

A dilatometry test was performed in a selected formulation of LWA to corroborate the expanding behaviour of the Clay-WTS LWA. The environmental impact was evaluated following the dynamic leaching test EN 12457-4 [52], to determine the potential release of heavy metal(loid)s in water. The leaching was conducted in a liquid-to-solid ratio of 10 L/kg for 24 h under agitation at 10 rpm. The leachate was filtered with a 0.45  $\mu\text{m}$  pore membrane, and the metallic elements were analysed by inductively coupled plasma mass spectrometry (ICP-MS), by using a NexION 350D from Perkin Elmer.

With regards to the formulated LWAC, flexural strength ( $\sigma_f$ ) was determined using the three points flexure test at 5 kg/s and  $\sigma_c$  was determined at 240 kg/s. Both  $\sigma_f$  and  $\sigma_c$  were measured using a universal testing machine Incotecnic MULTI-R1 applying an uniaxial load, according to the EN 196-1 [53]. A representative slice of LWAC was observed with of lenses to evaluate the cohesion between the cured cement and the LWA. The studied thermal properties for the LWAC were the thermal conductivity ( $\lambda$ ) and specific heat capacity ( $C_p$ ), both measured by a Quickline-30 Thermal Properties Analyzer equipment. The measurement method is based on the ASTM standard D5930 [54,55].

Table 4.- Methods summary table.

Materials and references		XRF	XRD	TGA	TOC	SSA	PSD	Dilatometry	WL	BI	$\rho_a$	Porosity	$\rho_{part}$	Water absorption	$\sigma_c$	Leaching	$\sigma_f$	$\lambda$	$C_p$
<b>Raw materials</b>	Clay	x	x	x	x	x	x	x								x			
	WTS	x	x	x	x	x	x	x								x			
<b>LWA</b>	0 wt.% WTS		x						x	x	x	x	x	x	x	x			
	2 wt.% WTS		x						x	x	x	x	x	x	x	x			
	5 wt.% WTS		x						x	x	x	x	x	x	x	x			
	7 wt.% WTS		x					x	x	x	x	x	x	x	x	x			
	10 wt.% WTS		x						x	x	x	x	x	x	x	x			
	13 wt.% WTS		x						x	x	x	x	x	x	x	x			
	15 wt.% WTS		x						x	x	x	x	x	x	x	x			
	20 wt.% WTS		x						x	x	x	x							
	50 wt.% WTS		x						x	x	x	x							
<b>LWAC</b>	LWAC 1										x				x		x	x	x
	LWAC 2										x				x		x	x	x

Symbols and abbreviations: XRF = X-ray fluorescence; XRD = X-ray diffraction; TGA = thermogravimetric analysis; SSA = specific surface area; PSD = particle size distribution; WL = weight loss; BI = bloating index;  $\rho_a$  = apparent density;  $\rho_{part}$  = particle density;  $\sigma_c$  = compressive strength;  $\sigma_f$  = flexural strength;  $\lambda$  = thermal conductivity;  $C_p$  = specific heat capacity.

### 3. Results and discussion

#### 3.1. Characterisation of clay and WTS

Table 5 compiles the chemical compositions of the two raw materials used determined by XRF. SiO<sub>2</sub> and Al<sub>2</sub>O<sub>3</sub> are the major compounds of the sludge and clay, although the content of Fe<sub>2</sub>O<sub>3</sub> in clay is also significant. The clay and WTS compositions determined from XRF data are plotted in Fig. 1. WTS composition plotted in the ternary diagram (black square) was outside the bloating area (dashed line zone). Accordingly, expansive natural clay was used to prepare clay-WTS formulations (grey triangles), which composition was inside of the bloating area. The expandability outside and at the limit of the bloating area were studied through a mixture of clay-WTS of 50 wt.% and 20 wt.% of WTS respectively.

Table 5.- Chemical composition results of clay and WTS determined by XRF.

	Weight %													
Sample	SiO <sub>2</sub>	Al <sub>2</sub> O <sub>3</sub>	Fe <sub>2</sub> O <sub>3</sub>	CaO	K <sub>2</sub> O	MgO	Na <sub>2</sub> O	ΣF*	MnO	P <sub>2</sub> O <sub>5</sub>	SO <sub>3</sub>	TiO <sub>2</sub>	Total	LOI**
Clay	57.30	15.00	8.93	2.47	4.62	3.91	0.27	20.20	-	-	0.13	1.31	93.94	6.06
WTS	13.74	29.38	2.12	2.04	0.86	0.58	0.20	5.80	0.16	1.55	-	0.16	50.81	49.19

\* ΣF = Fluxing oxides = Fe<sub>2</sub>O<sub>3</sub> + CaO + K<sub>2</sub>O + MgO + Na<sub>2</sub>O

\*\* Loss on ignition at 1,100 °C.

XRD spectra (presented as Fig. S2 in supplementary material) allowed the identification of the main crystalline phases. In the clay, quartz (SiO<sub>2</sub>, with very high intensity), kaolinite, muscovite and illite were the most intense phases. Chamosite, calcite, dolomite, hematite and potassium feldspar were also detected. In WTS, quartz and illite were the main phases, and small contents of halloysite, microcline, and anorthite were also detected. WTS exhibits a significant content of amorphous phases.

The thermal behaviour of clay and WTS was analysed through TGA. Fig. 2 shows the weight percentage and weight corrected heat flow in the temperature range of 20-1,200 °C. The total weight loss for clay was 8.4 % and for WTS 51.5 %. The first decomposition steps were attributed to water evaporation from adsorbed or weakly bonded water, at temperatures up to 200 °C [13]. The following

steps, with high percentages of weight loss in WTS, were associated with the hydroxides, and strongly bonded water decomposition, organic matter combustion (with strongly exothermic peaks in the heat flow signal for WTS), and carbonates decomposition (with an endothermic peak in the heat flow signal) [11,13,56,57]. The decompositions in both clay and WTS were mainly due to the high amount of bonded water and hydroxides. The high volume of gases produced by WTS was expected to maintain the bloating properties of clay with low substitution percentages. The TOC determined was 0.49 % in clay and 13.70 % in WTS (dry basis). There was a large content of hydroxides and hydrates in WTS that came from the coagulation and flocculation process in the drinking water treatment plant ( $\text{Al}(\text{OH})_3$ ), mainly because PACl was used as a coagulant. The organic matter detected in WTS mainly comes from two sources: flocculants added in the water treatment process, and matter dragged from the water source.

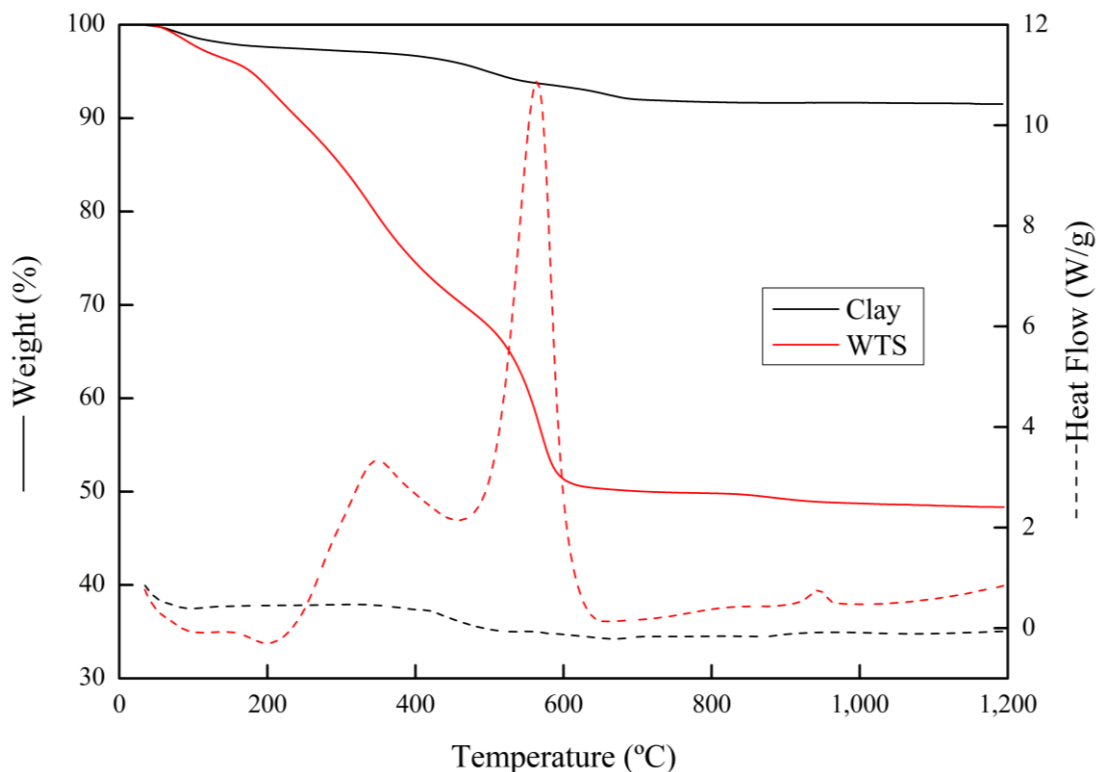


Fig. 2.- Weight and weight corrected heat flow of clay and WTS.

The specific BET surfaces results for clay and WTS (previously milled and sieved to the desired particle size) were  $36.7 \pm 0.2 \text{ m}^2/\text{g}$  and  $121.3 \pm 0.3 \text{ m}^2/\text{g}$ , respectively. The large values obtained

anticipate a good reactivity between the two raw materials. The high SSA also leads to high water absorption. About 30 % of water was needed to achieve the required workability to produce the unfired aggregates. The particle size of clay and WTS was suitable to produce LWA, with more than 90 % of particles below 80  $\mu\text{m}$ ,  $d_{90}$  of 32.0  $\mu\text{m}$  and 73.2  $\mu\text{m}$ , respectively.

A dilatometry test was performed up to 1,350 °C to determine the bloating properties of clay and WTS. The dimensional changes of clay (a) and WTS (b) are shown in Fig. 3. Because the reduction of the volume of clay is imperceptible up to 800 °C, this temperature was considered to be the starting temperature of the sintering process ( $T_{SS}$ ). From  $T_{SS}$ , the clay sample densifies to a maximum value, considered the end of sintering ( $T_{ES}$ ), ~1,160 °C. At temperatures higher than  $T_{ES}$  and to the end of the analysis, a softening phenomenon is perceptible, and the clay experiments a bloating to its maximum volume, temperature of maximum expansion ( $T_{ME}$ ), ~1,280 °C. This expansion occurs when part of the material is softened until a pyro-plastic impermeable phase is created which entraps the gases [20,58]. Finally, an increase of softening, and a decrease of viscosity leads to the melting [40]. The melting was not detected within the working temperature of 1,350 °C. For WTS, from the initial temperature to the end of the assay, the volume of the sample decreases. As shown in Fig. 3 (b), this process started at ~860 °C ( $T_{SS}$ ) until the end of the experiment at 1,350 °C. The melting of the sample was not detected either. WTS did not bloat as the viscosity of the material at high temperature was probably not large enough to trap the released gases [20]. The volume variation for both samples,  $T_{SS}$ ,  $T_{ES}$  and  $T_{ME}$  are plotted in Fig. 4. In addition, the volume variation of a mixture of clay with a 7 wt.% WTS is also shown because this mixture was used to develop the LWAC 2 (as will be discussed later). The plotted volume change of the mixture has almost the same characteristic temperatures ( $T_{SS}$ ,  $T_{ES}$  and  $T_{ME}$ ) than clay, and the expansion process is very similar, which indicates that the bloating properties of mixtures with 7 wt.% of WTS are suitable for the LWAC production (see next section).



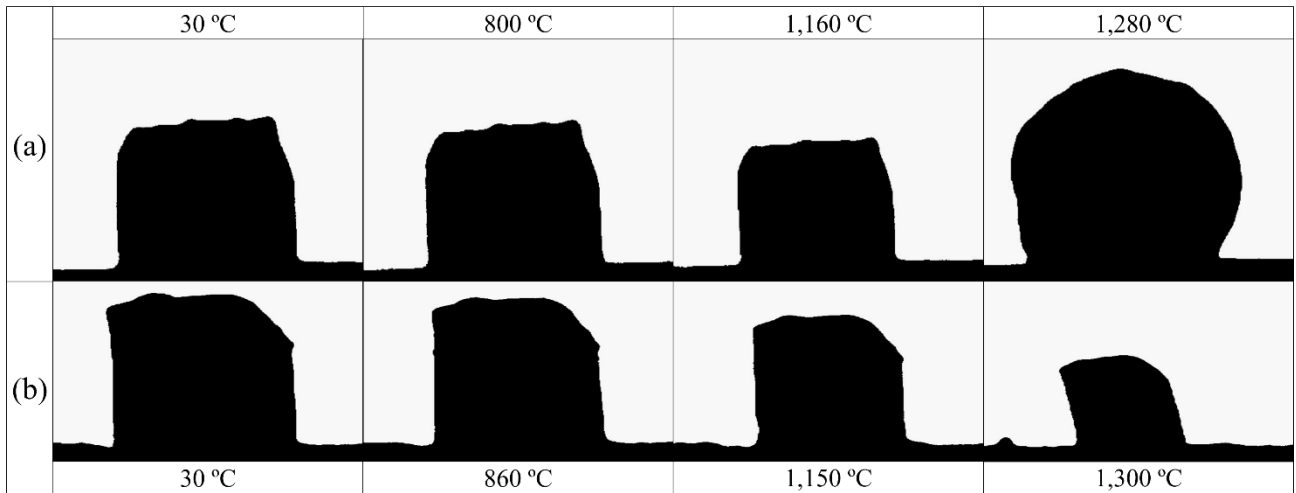


Fig. 3.- Images of clay (a) and WTS (b) during dilatometry test at different characteristic temperatures.

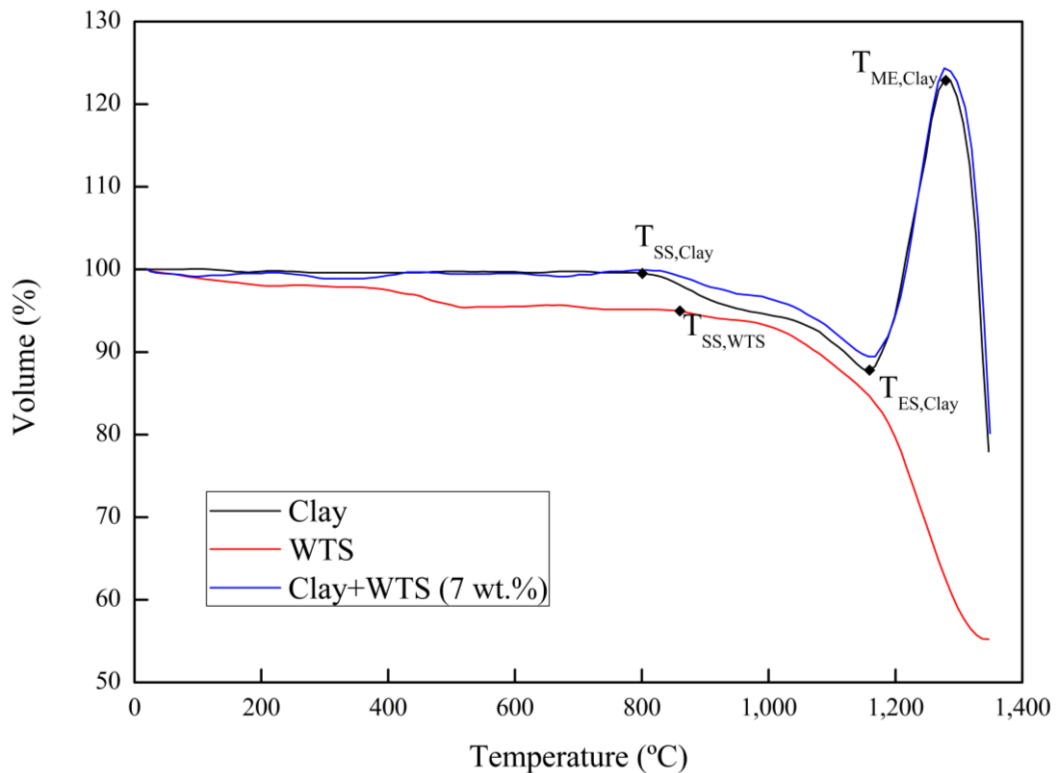


Fig. 4.- Volume % versus temperature from dilatometry test for clay, WTS and Clay-WTS 7 wt.% mixture.

### 3.2. Properties of LWA

As expected from the bloating diagram (Fig. 1) and confirmed with dilatometry (Fig. 3 (b) and Fig. 4), WTS did not present bloating properties. Therefore, nine formulations with different percentages

of WTS replacing clay were prepared from 0 wt.% to 50 wt.% (Table 1). The weight loss (WL) during the sintering process of the unfired aggregates is shown in Fig. 5. The measurement was performed on 25 samples of each formulation. A linear increase of WL was detected with increasing WTS percentage, with a good coefficient of determination ( $R^2=0.97$ ) between WL and WTS percentage. This increase is due to the high WL of WTS, observed in TGA (Fig. 2). The WL detected in aggregates without WTS ( $8.8 \pm 0.4$  %), agreed with the total weight loss of clay detected in TGA analysis (8.4 %).

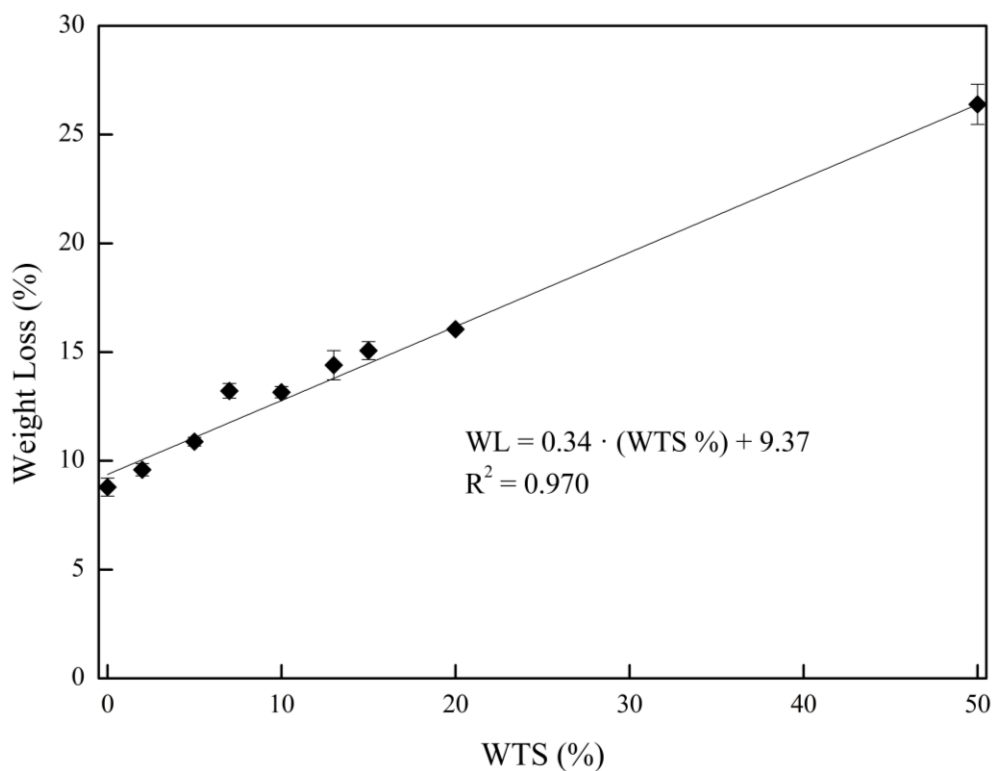


Fig. 5.- Weight Loss after the sintering process at 1,175 °C for 8 min versus WTS percentage.

The bloating index (BI) results of 25 samples of LWA presented in Fig. 6 (a) revealed an exponential decrease of expansion of unfired LWA after the sintering process ( $R^2 \sim 1$ ). The decrease supports the hypothesis extracted from Fig. 1, that WTS (outside of the bloating area) reduced the bloating properties of clay. This reduction was due to the change of composition, which probably results in lower viscosity of the shell during the firing process, hence the gases inside the aggregate would be released. As expected, LWA with 0 wt.% of WTS exhibited the highest values of BI (450 %

of expansion), and being LWA produced with 50 wt.% of WTS the lowest. Actually, LWA with this formulation did not suffer expansion during the sintering, but rather a contraction (25 %), because the formulation was at the outside of the bloating area. Apparent densities ( $\rho_a$ ) of 25 LWA are also shown in Fig. 6 (a).  $\rho_a$  results also presented an exponential trend increasing with WTS addition ( $R^2=0.98$ ). The bloating was lower for the LWA with higher WTS content; therefore, more compact and denser LWA were obtained. These results were confirmed by means of the porosity study through image treatment (ImageJ). LWA with higher WTS content presented lower porosity. The porosity data followed an exponential trend ( $R^2=0.95$ ), as shown in Fig. 6 (b). As aforementioned, the decrease of porosity with an increase of WTS substitution was probably due to the change in the viscosity of the raw materials during the heating process. With less viscous phases, the volatile compounds formed from the thermal decomposition could escape from the aggregate, reducing the porosity and the bloating, and increasing the density. The bloating decrease is clearly observed in Fig. 7, where fired aggregates of the nine formulations are imaged after a heating treatment for 8 min at 1,175 °C. The sizes of the unfired specimens were similar (~10 mm). The external surface of LWA with 0 and 2 wt.% of sludge did not present a vitreous, but rather a wrinkled aspect. LWA with more than 5 wt.% of WTS presented a vitreous external phase. Aggregates with higher WTS content, ~10-15 wt.%, presented a cracked external aspect, probably due to the thermal shock and to the high amount of gases released from WTS. Unfired aggregates with higher WTS content presented also higher weight loss during the sintering. The fast release of a large volume of gases fissured the brittle external structure of these LWA.

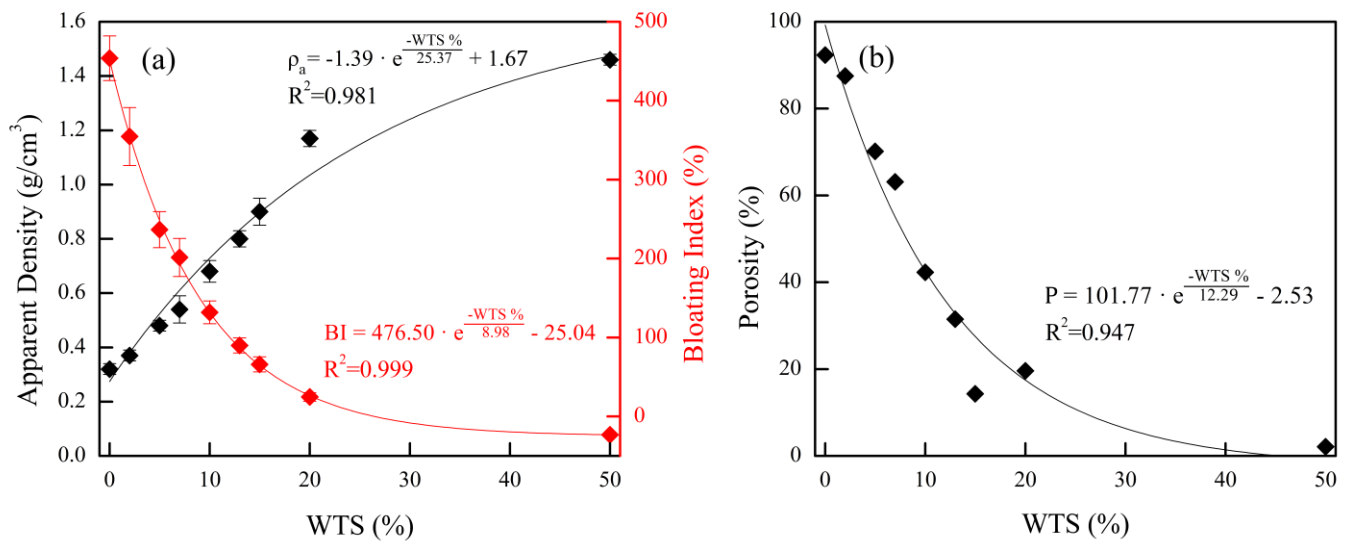


Fig. 6.- Bloating Index and Apparent Density (a) and Porosity (b) after the sintering process at 1,175 °C for 8 min versus WTS percentage.

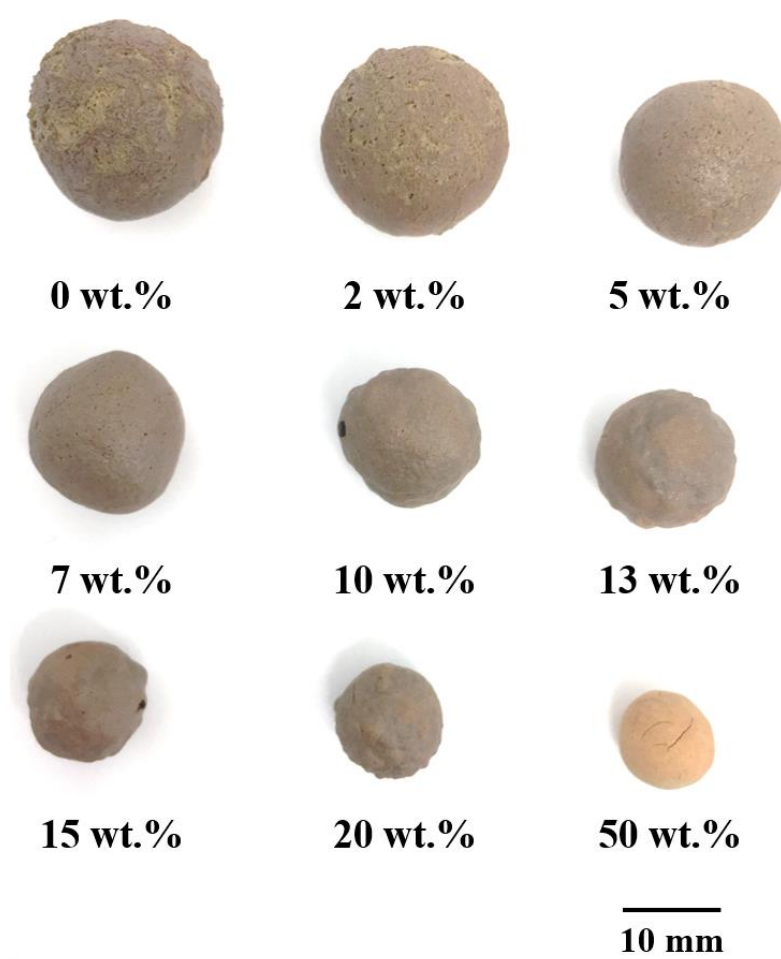


Fig. 7.- Image of fired LWA with different WTS percentage.

Taking into account the results of BI, porosity and  $\rho_a$ , formulations with 20 wt.% WTS and 50 wt.% WTS were discarded to be used as LWA. Indeed, 20 wt.% WTS led to a very low expansion (around 25 %), while 50 wt.% WTS formulations exhibited a shrinkage. Hence, only percentages up to 15 wt.% WTS were further studied. Fig. 8 shows a linear increase in the particle density ( $\rho_{part}$ ) of LWA with percentage of WTS, as a result of the lower volume of gases captured inside the aggregates, since they were released during the sintering. Denser aggregates are formed when compared to LWA without WTS. The  $\rho_{part}$  trend is linear in the range 0-15 wt.% WTS. The water absorption measured for the LWA was between 13 and 19 %. Although the porosity and the density followed a trend with increasing WTS content, water absorption did not follow such a trend. This behaviour is due to the outer layer of some aggregates, which presented cracks and regions with different permeability, causing different water absorption on the aggregates despite their porosity. Water absorption is an important parameter because, during the concrete ageing, aggregates with high water absorption can capture the needed water for the cement setting.

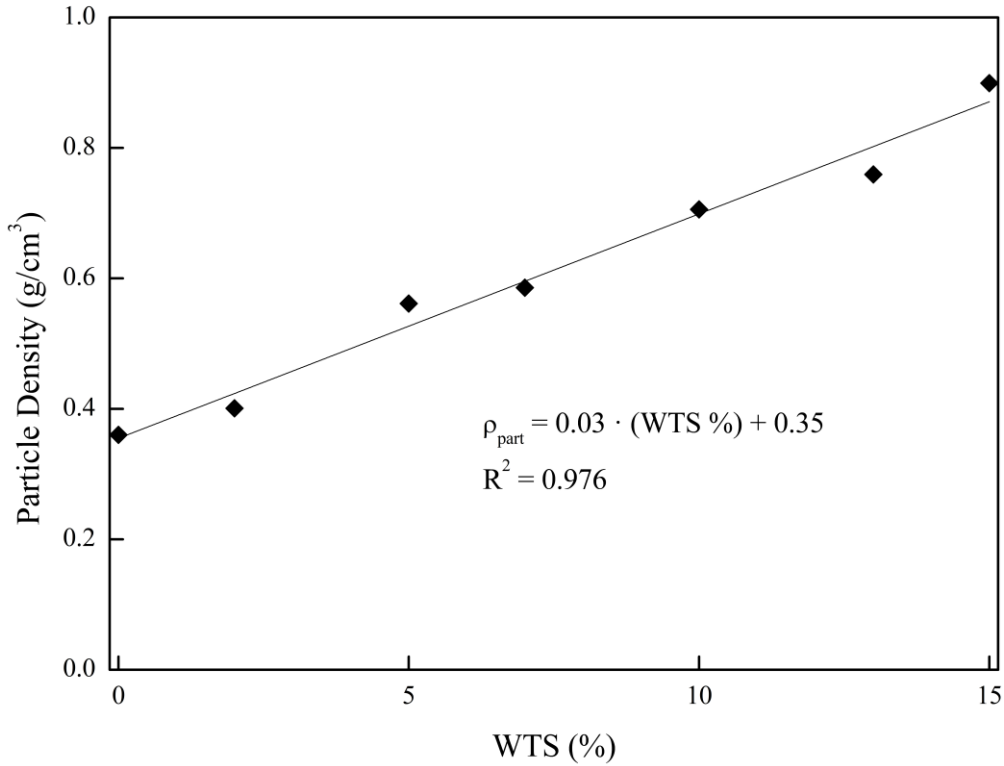


Fig. 8.- Particle density of LWA with percentages of WTS from 0 to 15 wt.%.

Twelve LWA were studied by means of compression tests. Fig. 9 (a) shows the compressive strength ( $\sigma_c$ ) of the LWA as a function of WTS content.  $\sigma_c$  increased with the WTS addition (as expected from the previous data). When the sludge substituted the clay, the bloating of the aggregates was lower, and thus more compact and denser LWA were obtained. A number of aggregates with percentages of WTS higher than 7-10 wt.% presented a cracked external surface. The cracks acted as stress riser, causing the compressive strength of these aggregates to be lower, therefore a large dispersion of compressive strength results was obtained for the LWA with large WTS percentages. The specific compressive strength ( $\sigma_c/\rho$ ) is plotted in Fig. 9 (b), where the highest value corresponds to 10 wt.% of WTS, and the trend of the results is different than  $\sigma_c$ . The characterization of the LWA through XRD (supplementary material Fig. S3) revealed the presence of two main crystalline phases: quartz ( $\text{SiO}_2$ ) and hercynite ( $\text{FeAl}_2\text{O}_4$ ). Increasing the WTS content, two new crystalline phases were

detected with increasing intensity: mullite ( $\text{Al}_6\text{Si}_2\text{O}_{13}$ ) and anorthite ( $\text{CaAl}_2\text{Si}_2\text{O}_8$ ). Also, the intensity of several quartz peaks decreased with increasing WTS addition. These new aluminium-rich crystalline phases are formed due to the high aluminium content in WTS, as revealed by XRF (see Table 5). All the crystalline phases containing  $\text{H}_2\text{O}$  and  $\text{OH}^-$  detected in raw materials are no longer present or they have transformed into new non-hydrated phases during the firing process. In the X-ray spectra of all LWA, the presence of amorphous phases was detected. Considering the results for the different formulations, we selected LWA with 7 wt.% WTS for a preliminary study for its application in LWAC.

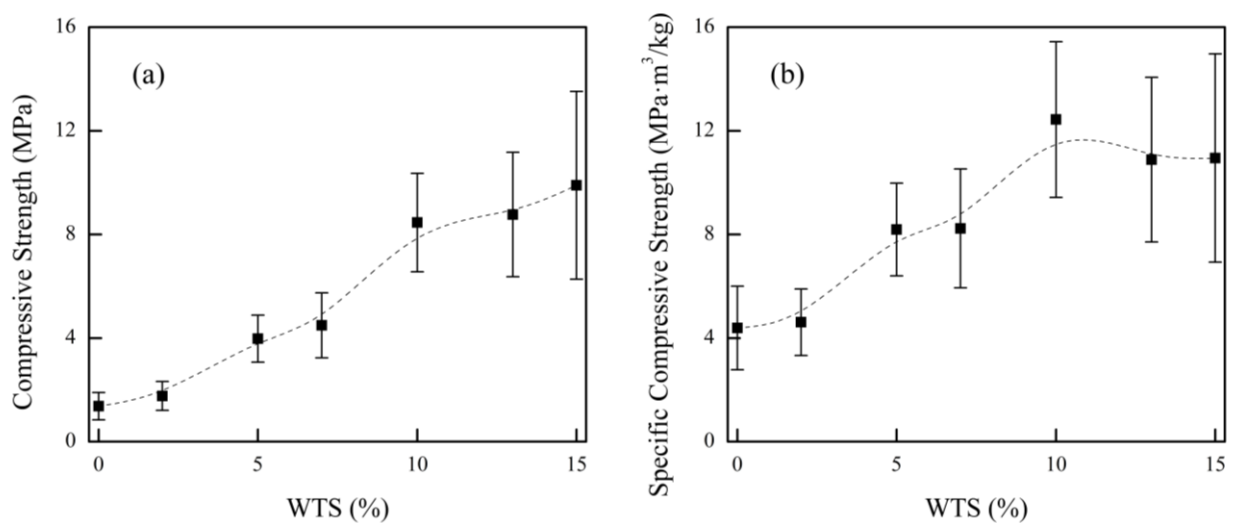


Fig. 9.- Compressive strength (a) and specific compressive strength (b) results for the sintered LWA based on the WTS added.

### 3.3. Leaching impact assessment

Leaching tests were performed to determine the potential environmental impact. The analysis was conducted for both raw materials and for the LWA with different percentages of WTS substituting clay (up to 15 wt.%). Table 6 shows the leaching results as well as the regulatory limits according to the European Commission legislation. Broken LWA (< 10 mm), clay and WTS (< 80  $\mu\text{m}$ ) were used to perform the leaching test. The pH of LWA is larger than in raw materials, due to the formation of alkali oxides generated during the thermal decomposition of carbonates. It should be noted that as the wt.%

WTS in the LWA increases, the pH decreases, probably due to the decrease in alkali earth oxides and the increase in alumina that would control pH. Both raw materials and LWA released heavy metal(loid)s in the leachates below the regulatory limits established by the European Commission for a secondary materials reuse, making them suitable for this purpose. The small differences between the LWA with different formulations were more likely due to the heterogeneity of the raw materials than to the differences in the formulation of the aggregates.

LWA with sludge replacing higher than 5 wt.% presented a very good water resistance, as the water in the leachates was transparent and without suspended particles. In contrast, leachates of LWA with less percentage of WTS were slightly turbid (higher concentration of suspended particles). This behaviour suggested some deterioration of the aggregates in contact with water. For the aggregates with percentages up to 5 wt.%, this effect was due to the lack of an external vitreous layer that waterproofs the inner of the aggregates, as observed in Fig. 7.



Table 6.- Leaching results following the EN 12457-4 standard (mg/kg).

	Clay	WTS	LWA 0 wt.% WTS	LWA 2 wt.% WTS	LWA 5 wt.% WTS	LWA 7 wt.% WTS	LWA 10 wt.% WTS	LWA 13 wt.% WTS	LWA 15 wt.% WTS	Inert limit*	Non- hazardous limit*	Hazardous limit*
<b>pH</b>	8.09	8.59	9.16	9.03	8.85	8.56	8.47	8.31	8.19	-	-	-
<b>As</b>	0.121	0.006	0.440	0.443	0.481	0.417	0.424	0.376	0.290	0.5	2	25
<b>Ba</b>	0.149	0.682	0.124	0.135	0.079	0.153	0.070	0.067	0.066	20	100	300
<b>Cd</b>	<0.001	<0.001	<0.001	<0.001	<0.001	<0.001	<0.001	<0.001	<0.001	0.04	1	5
<b>Cr</b>	0.004	0.013	0.003	<0.001	<0.001	0.002	<0.001	<0.001	<0.001	0.5	10	70
<b>Cu</b>	0.279	0.040	0.092	0.150	0.345	0.087	0.031	0.054	<0.001	2	50	100
<b>Fe</b>	0.146	0.113	0.100	0.068	0.033	0.113	0.031	0.015	0.014	-	-	-
<b>Hg</b>	<0.002	<0.005	<0.002	<0.002	<0.002	<0.002	<0.002	<0.002	<0.002	0.01	0.2	2
<b>Mn</b>	0.067	3.382	0.107	0.012	0.012	0.040	0.020	0.032	0.033	-	-	-
<b>Mo</b>	0.040	0.005	0.027	0.028	0.030	0.025	0.020	0.019	0.014	0.5	10	30
<b>Ni</b>	0.005	0.040	0.055	0.005	0.009	0.006	0.006	0.004	0.069	0.4	10	40
<b>Pb</b>	0.002	0.016	0.029	<0.001	0.019	0.009	0.006	0.031	<0.001	0.5	10	50
<b>Se</b>	0.022	<0.01	<0.02	<0.02	<0.02	<0.02	<0.02	<0.02	<0.02	0.1	0.5	7
<b>Sn</b>	<0.001	<0.002	<0.001	<0.001	<0.001	<0.001	<0.001	<0.001	<0.001	-	-	-
<b>Te</b>	<0.001	<0.002	<0.001	<0.001	<0.001	<0.001	<0.001	<0.001	<0.001	-	-	-
<b>Zn</b>	0.048	0.113	0.275	<0.02	0.201	<0.02	<0.02	0.380	<0.02	4	50	200

\* Regulatory limits according to European Commission.

### 3.4. LWAC results

The LWA selected for producing LWAC 2 contains 7 wt.% of WTS, because of its properties of bloating, density, and porosity were similar enough to LWA with 0 wt.% of WTS. Furthermore the water resistance for this composition was better than in LWA with lower WTS additions. The results for both LWAC are compared in Table 7 to other types of lightweight concretes from literature. The densities of LWAC 1 and LWAC 2 were similar, and approximately half of a mass concrete density. Since LWA densities are low, the density of LWAC is also lower than that of the conventional concrete. As the density of LWAC 1 and LWAC 2 are similar, it can be concluded that the aggregates with 7 wt.% of WTS can be used in LWAC maintaining essentially the same density. The densities of LWAC 1 and LWAC 2 were lower than most of the LWAC reported in the literature as only LWA were used as aggregates, to achieve higher thermal resistivity [59,60]. The densities obtained for our LWAC are even comparable to several foamed concretes [61].

Table 7.- Mechanical and thermal properties of LWAC.

Property	LWAC 1	LWAC 2	Foam concrete* [61]	Foam expanded clay concrete [62]	Structural LWAC** [63]
$\rho_a$ (kg/m <sup>3</sup> )	1,064	1,094	1,000	600	1,600
$\sigma_f$ (MPa)	0.8 ± 0.3	1.0 ± 0.2	-	-	-
$\sigma_c$ (MPa)	4.9 ± 0.1	4.7 ± 0.7	2.5-3.0	4.7	17.0
$\lambda$ (W/m·K)	0.42 ± 0.04	0.49 ± 0.02	0.23-0.30	0.15-0.20	-
$C_p$ (J/kg·K)	1,370 ± 233	1,446 ± 87	-	-	-

\* Cellular concrete properties with respect to density of 1,000 kg/m<sup>3</sup>.

\*\* Minimum  $\sigma_c$  value for structural concrete produced with only LWA for a maximum density of 1,600 kg/m<sup>3</sup>.

The mechanical properties in terms of flexural strength ( $\sigma_f$ ) and compressive strength ( $\sigma_c$ ) of LWAC 1 and LWAC 2 are also presented in Table 7. The minimum  $\sigma_c$  of a structural LWAC defined by ASTM C330 is 17 MPa, for a LWAC with a density of 1,600 kg/m<sup>3</sup> formulated only with LWA [63]. The strength of LWAC 1 and LWAC 2 is much lower than the minimum value for structural LWAC, but this is mainly due to their low density. The mechanical properties obtained for the LWAC were much lower than mass concrete, as the LWA resistance is much lower than normal weight

aggregates (e.g. sand) due to the inner porosity [64]. The formulation of the concretes in this study was carried out only with LWA, without sand. As a consequence, the  $\sigma_c$  of LWAC 1 and LWAC 2 were also much lower than most of the LWAC reported in the literature that used sand or other fine aggregate in addition to expanded clay coarse aggregates [59]. When sand is added as a filler,  $\sigma_c$  increases [25]. Compared to foam concrete from Table 7, for a similar density, the LWAC from this work presented a higher  $\sigma_c$ . The strength is comparable to foam LWAC from literature [62]. Comparing LWAC 1 to LWAC 2, it may be seen that their resistance to flexion and compression were very similar. Thus, the substitution of clay by WTS did not modify the mechanical properties of the produced concrete. This result is important because it means that the LWA with WTS is suitable to produce LWAC without losing mechanical properties.

Table 7 shows that thermal conductivity ( $\lambda$ ) and specific heat capacity ( $C_p$ ) for LWAC are much lower and higher than mass concrete, respectively. The results of  $\lambda$  are lower than for most of LWAC [65], as well as lower than other LWAC formulated with WTS LWA and normal weight aggregates [66]. The  $\lambda$  are higher than foam concrete with similar densities ( $1,000 \text{ kg/m}^3$ ), but comparable to cellular concretes with densities of  $1,200\text{-}1,400 \text{ kg/m}^3$  [61]. Thermal conductivity of foam LWAC is lower, since the density is also much lower. Moreover,  $\lambda$  and  $C_p$  of LWAC 2 were similar to the properties of LWAC 1. The decrease of  $\lambda$  and the increase of  $C_p$  are the direct consequence of incorporating LWA (with a highly porous structure) instead of normal weight aggregates. This means that the higher volume of air inside the concrete reduces  $\lambda$ , which leads to a thermal insulation improvement in building application and to an increase in energy efficiency. Therefore, the developed materials in this study can be mainly used in facades and signs [25].

The cohesion of LWA with cement paste was evaluated by studying the part between the aggregates and the cement paste bulk by means of optical microscopy. There is no separation between the cement matrix and the aggregates; the desired cohesion in both LWAC was obtained. In both

concretes, mainly in the largest LWA, the cement paste slightly diffuses into the aggregate shell. This phenomenon was also observed in other LWAC produced with expanded clay [67,68]. Furthermore, a change of colour around the aggregates was observed, probably due to an interaction between the cement matrix and the aggregates. This change could be attributed to a modification of the morphology, however a more deeply study must be done to fully understand the morphology in the aggregate-cement zone.

#### **4. Conclusions**

We have analysed the possibility of valorising WTS by producing LWA, giving this waste an added value. LWA with mixtures of expanded clay and WTS (from 0 to 50 wt.% of WTS) were formulated, and their properties were characterised. A preliminary test of producing LWAC was also performed. Two LWAC were formulated: one with commercial LWA (LWAC 1) and another with a mixture of fine commercial LWA and coarse LWA of a selected composition from this project (LWAC 2). The properties of both LWAC were analysed. The following main conclusions were extracted from this work:

- Introducing a waste with not expanding properties reduces the expandability of the clay, therefore reducing its porosity and increasing its density. However, it is possible to produce LWA with mixtures of expanded clay and WTS with low substitution percentages (<15 wt.%), obtaining high porosity and bloating index, and low densities. Therefore, WTS can be valorised in the LWA production.
- High percentages of substitution (>20 wt.% of WTS) led to LWA with poor properties. Aggregates formulated with only WTS did not experiment bloating, despite its high thermal weight loss, due to the composition of WTS.

- The environmental impact of the aggregates containing WTS, assessed through leaching test, revealed that the concentration of heavy metals and metalloids were far below the hazardous limits established by the European Commission.
- The preliminary study of LWAC was successful. Both LWAC presented low densities and thermal conductivities. As expected for the large amount of LWA and the lack of fine aggregates, the mechanical properties in terms of compressive strength and flexural strength were low.
- All the properties of LWAC 2, which contains LWA with 7 wt.% of WTS, were essentially the same as those of LWAC 1, formulated with commercial LWA. This result reinforces the conclusion that WTS can be valorised in LWA production.

This work presents the possibility of valorising WTS for the LWA production. However, testing different formulations of LWAC using LWA with different percentages of WTS, and introducing other variables not studied in this work (e.g. additives and fine aggregate) would increase the reliability of the obtained results. The future trends of research should focus on finding the optimal formulation for LWAC manufacturing maximizing WTS content.

### **Acknowledgements**

The authors would like to thank the Catalan Government for the quality accreditation given to their research group DIOPMA (2017 SGR 118). Authors also thank Leca International Company for supplying the expanded clay and commercial lightweight aggregates and FAE Company for the dilatometry tests performed in their facilities.

### **Funding**

The authors would like to thank the companies SORIGUÉ and NORDVERT S.L. for their financial support and for providing access to sampling sites. Mr. Alex Maldonado-Alameda and Mr. Jofre Mañosa are grateful to the Catalan Government for their research Grants, FI-DGR 2017 and FI 2020, respectively. Dr. Jessica Giro-Paloma is a Serra Hünter Fellow.

## References

- [1] J. Giro-Paloma, J. Mañosa, A. Maldonado-Alameda, M.J. Quina, J.M. Chimenos, Rapid sintering of weathered municipal solid waste incinerator bottom ash and rice husk for lightweight aggregate manufacturing and product properties, *J. Clean. Prod.* 232 (2019) 713–721. <https://doi.org/10.1016/j.jclepro.2019.06.010>.
- [2] T. Ahmad, K. Ahmad, M. Alam, Sustainable management of water treatment sludge through 3 ‘R’ concept, *J. Clean. Prod.* 124 (2016) 1–13. <https://doi.org/10.1016/j.jclepro.2016.02.073>.
- [3] T. Ahmad, K. Ahmad, M. Alam, Characterization of Water Treatment Plant’s Sludge and its Safe Disposal Options, *Procedia Environ. Sci.* 35 (2016) 950–955. <https://doi.org/10.1016/j.proenv.2016.07.088>.
- [4] E. Nimwinya, W. Arjharn, S. Horpibulsuk, A sustainable calcined water treatment sludge and rice husk ash geopolymer, *J. Clean. Prod.* 119 (2016) 128–134. <https://doi.org/10.1016/j.jclepro.2016.01.060>.
- [5] T.K. Trinh, L.S. Kang, Response surface methodological approach to optimize the coagulation – flocculation process in drinking water treatment., *Chem. Eng. Res. Des.* 89 (2011) 1126–1135. <https://doi.org/10.1016/j.cherd.2010.12.004>.
- [6] A.O. Babatunde, Y.Q. Zhao, Constructive approaches towards water treatment works sludge management: An international review of beneficial re-uses, *Crit. Rev. Environ. Sci. Technol.* 37 (2007) 129–164. <https://doi.org/10.1080/10643380600776239>.
- [7] A.T. Nair, M.M. Ahammed, The reuse of water treatment sludge as a coagulant for post-treatment of UASB reactor treating urban wastewater, *J. Clean. Prod.* 96 (2015) 272–281. <https://doi.org/10.1016/j.jclepro.2013.12.037>.
- [8] F. Arteaga, L.V. Cremades, J.A. Cusidó, Recycling of sludge from drinking water treatment as ceramic material for the manufacture of tiles, *J. Clean. Prod.* 201 (2018) 1071–1080. <https://doi.org/10.1016/j.jclepro.2018.08.094>.
- [9] M.O. Ramadan, H.A. Fouad, A.M. Hassanain, Reuse of Water Treatment Plant Sludge in Brick Manufacturing, *J. Appl. Sci. Res.* 4 (2008) 1223–1229.
- [10] H.X. Chen, X. Ma, H.J. Dai, Reuse of water purification sludge as raw material in cement production, *Cem. Concr. Compos.* 32 (2010) 436–439. <https://doi.org/10.1016/j.cemconcomp.2010.02.009>.
- [11] M.T. Blanco-varela, N.H. Rodríguez, S. Martínez Ramírez, Validity of water industry wastes in cement industry, *Civ. Environ. Res.* 4 (2013) 27–30.
- [12] R.H. Geraldo, L.F.R. Fernandes, G. Camarini, Water treatment sludge and rice husk ash to sustainable geopolymer production, *J. Clean. Prod.* 149 (2017) 146–155. <https://doi.org/10.1016/j.jclepro.2017.02.076>.
- [13] C. Ferone, I. Capasso, A. Bonati, G. Roviello, F. Montagnaro, L. Santoro, R. Turco, R. Ciof, Sustainable management of water potabilization sludge by means of geopolymers production, *J. Clean. Prod.* 229 (2019) 1–9.
- [14] X. Guan, G. Chen, C. Shang, Re-use of water treatment works sludge to enhance particulate pollutant removal from sewage, *Water Res.* 39 (2005) 3433–3440.

<https://doi.org/10.1016/j.watres.2004.07.033>.

- [15] S. Cao, D. Zheng, E. Yilmaz, Z.Y. Yin, G.L. Xue, F.D. Yang, Strength development and microstructure characteristics of artificial concrete pillar considering fiber type and content effects, *Constr. Build. Mater.* 256 (2020) 119408. <https://doi.org/10.1016/j.conbuildmat.2020.119408>.
- [16] R. Sharma, R.A. Khan, Sustainable use of copper slag in self compacting concrete containing supplementary cementitious materials, *J. Clean. Prod.* 151 (2017) 179–192. <https://doi.org/10.1016/j.jclepro.2017.03.031>.
- [17] B. Ayati, V. Ferrándiz-Mas, D. Newport, C. Cheeseman, Use of clay in the manufacture of lightweight aggregate, *Constr. Build. Mater.* 162 (2018) 124–131. <https://doi.org/10.1016/j.conbuildmat.2017.12.018>.
- [18] M. Sarıdemir, S. Çelikten, Investigation of fire and chemical effects on the properties of alkali-activated lightweight concretes produced with basaltic pumice aggregate, *Constr. Build. Mater.* 260 (2020). <https://doi.org/10.1016/j.conbuildmat.2020.119969>.
- [19] J.A. Bogas, D. Cunha, Non-structural lightweight concrete with volcanic scoria aggregates for lightweight fill in building's floors, *Constr. Build. Mater.* 135 (2017) 151–163. <https://doi.org/10.1016/j.conbuildmat.2016.12.213>.
- [20] M. Dondi, P. Cappelletti, M.D. Amore, R. De Gennaro, S.F. Graziano, A. Langella, M. Raimondo, C. Zanelli, Lightweight aggregates from waste materials: Reappraisal of expansion behavior and prediction schemes for bloating, *Constr. Build. Mater.* 127 (2016) 394–409. <https://doi.org/10.1016/j.conbuildmat.2016.09.111>.
- [21] M.J. Quina, J.M. Bordado, R.M. Quinta-ferreira, Recycling of air pollution control residues from municipal solid waste incineration into lightweight aggregates, *Waste Manag.* 34 (2014) 430–438. <https://doi.org/10.1016/j.wasman.2013.10.029>.
- [22] T. Uygunog, Investigation of properties of low-strength lightweight concrete for thermal insulation, *Build. Environ.* 42 (2007) 584–590. <https://doi.org/10.1016/j.buildenv.2005.09.024>.
- [23] B. Zhang, C.S. Poon, Use of Furnace Bottom Ash for producing lightweight aggregate concrete with thermal insulation properties, *J. Clean. Prod.* 99 (2015) 94–100. <https://doi.org/10.1016/j.jclepro.2015.03.007>.
- [24] P. Shafigh, M.A. Nomeli, U.J. Alengaram, H. Bin Mahmud, Engineering properties of lightweight aggregate concrete containing limestone powder and high volume fly ash, *J. Clean. Prod.* 135 (2016) 148–157. <https://doi.org/10.1016/j.jclepro.2016.06.082>.
- [25] F. Pelisser, A. Barcelos, D. Santos, M. Peterson, A.M. Bernardin, Lightweight concrete production with low Portland cement consumption, *J. Clean. Prod.* 23 (2012) 68–74. <https://doi.org/10.1016/j.jclepro.2011.10.010>.
- [26] Y. Geng, W. Ji, Z. Wang, B. Lin, Y. Zhu, A review of operating performance in green buildings: Energy use, indoor environmental quality and occupant satisfaction, *Energy Build.* 183 (2019) 500–514. <https://doi.org/10.1016/j.enbuild.2018.11.017>.
- [27] B. Ayati, C. Molineux, D. Newport, C. Cheeseman, Manufacture and performance of lightweight aggregate from waste drill cuttings, *J. Clean. Prod.* 208 (2019) 252–260.

<https://doi.org/10.1016/j.jclepro.2018.10.134>.

- [28] A. Mueller, S.N. Sokolova, V.I. Vereshagin, Characteristics of lightweight aggregates from primary and recycled raw materials, *Constr. Build. Mater.* 22 (2008) 703–712. <https://doi.org/10.1016/j.conbuildmat.2007.06.009>.
- [29] C.M. Riley, Relation of Chemical Properties to the Bloating of Clays, *J. Am. Ceram. Soc.* 34 (1951) 121–128.
- [30] R. De Gennaro, P. Cappelletti, G. Cerri, M. De Gennaro, M. Dondi, A. Langella, Zeolitic tuffs as raw materials for lightweight aggregates, 25 (2004) 71–81. <https://doi.org/10.1016/j.clay.2003.08.005>.
- [31] M. Moreno-Maroto, M. Uceda-Rodríguez, C.J. Cobo-ceacero, M. Calero de Hoces, M.Á. MartínLara, T. Cotes-Palomino, A.B. López García, C. Martínez-García, Recycling of ‘alperujo’ (olive pomace) as a key component in the sintering of lightweight aggregates, *J. Clean. Prod.* 239 (2019). <https://doi.org/10.1016/j.jclepro.2019.118041>.
- [32] M. Franus, R. Panek, J. Madej, W. Franus, The properties of fly ash derived lightweight aggregates obtained using microwave radiation, *Constr. Build. Mater.* 227 (2019) 1–10. <https://doi.org/10.1016/j.conbuildmat.2019.116677>.
- [33] G.P. Lyra, V. dos Santos, B.C. De Santis, R.R. Rivaben, C. Fischer, E.M. de J.A. Pallone, J.A. Rossignolo, Reuse of sugarcane bagasse ash to produce a lightweight aggregate using microwave oven sintering, *Constr. Build. Mater.* 222 (2019) 222–228. <https://doi.org/10.1016/j.conbuildmat.2019.06.150>.
- [34] Y. Cao, R. Liu, Y. Xu, F. Ye, R. Xu, Y. Han, Effect of SiO<sub>2</sub>, Al<sub>2</sub>O<sub>3</sub> and CaO on characteristics of lightweight aggregates produced from MSWI bottom ash sludge (MSWI-BAS), *Constr. Build. Mater.* 205 (2019) 368–376. <https://doi.org/10.1016/j.conbuildmat.2019.01.104>.
- [35] X. Li, C. He, Y. Lv, S. Jian, G. Liu, W. Jiang, D. Jiang, Utilization of municipal sewage sludge and waste glass powder in production of lightweight aggregates, *Constr. Build. Mater.* 256 (2020) 119413. <https://doi.org/10.1016/j.conbuildmat.2020.119413>.
- [36] C. Huang, S. Wang, Application of water treatment sludge in the manufacturing of lightweight aggregate, *Constr. Build. Mater.* 43 (2013) 174–183. <https://doi.org/10.1016/j.conbuildmat.2013.02.016>.
- [37] F. Messina, C. Ferone, A. Molino, G. Roviello, F. Colangelo, B. Molino, R. Cioffi, Synergistic recycling of calcined clayey sediments and water potabilization sludge as geopolymer precursors: Upscaling from binders to precast paving cement-free bricks, *Constr. Build. Mater.* 133 (2017) 14–26. <https://doi.org/10.1016/j.conbuildmat.2016.12.039>.
- [38] O. Kizinievič, R. Žurauskiene, V. Kizinievič, R. Žurauskas, Utilisation of sludge waste from water treatment for ceramic products, *Constr. Build. Mater.* 41 (2013) 464–473. <https://doi.org/10.1016/j.conbuildmat.2012.12.041>.
- [39] European Committee for Standardization, EN 14899: Characterization of waste. Sampling of waste materials. Framework for the preparation and application of a sampling plan., (2005).
- [40] M.J. Quina, M.A. Almeida, R. Santos, J.M. Bordado, R.M. Quinta-Ferreira, Compatibility analysis of municipal solid waste incineration residues and clay for producing lightweight



- aggregates, *Appl. Clay Sci.* 102 (2014) 71–80. <https://doi.org/10.1016/j.clay.2014.10.016>.
- [41] American Society for Testing and Materials, *ASTM C125: Standard Terminology Relating to Concrete and Concrete Aggregates*, (2007).
- [42] W. Fuller, S.E. Thompson, The laws of proportioning concrete, *Trans. Am. Soc. Civ. Eng.* (1907) 67–143.
- [43] O. Ginés, J.M. Chimenos, A. Vizcarro, J. Formosa, J.R. Rosell, Combined use of MSWI bottom ash and fly ash as aggregate in concrete formulation: Environmental and mechanical considerations, *J. Hazard. Mater.* 169 (2009) 643–650. <https://doi.org/10.1016/j.jhazmat.2009.03.141>.
- [44] Y. Zhao, J. Gao, F. Chen, C. Liu, X. Chen, Utilization of waste clay bricks as coarse and fine aggregates for the preparation of lightweight aggregate concrete, *J. Clean. Prod.* 201 (2018) 706–715. <https://doi.org/10.1016/j.jclepro.2018.08.103>.
- [45] A.A. Aliabdo, A.E.M. Abd-Elmoaty, H.H. Hassan, Utilization of crushed clay brick in concrete industry, *Alexandria Eng. J.* 53 (2014) 151–168. <https://doi.org/10.1016/j.aej.2013.12.003>.
- [46] B. Zhang, C.S. Poon, Sound insulation properties of rubberized lightweight aggregate concrete, *J. Clean. Prod.* 172 (2018) 3176–3185. <https://doi.org/10.1016/j.jclepro.2017.11.044>.
- [47] C. Jones, D. Goad, W.M. Hale, Examining soaking duration of coarse clay and shale lightweight aggregates for internal curing in conventional concrete, *Constr. Build. Mater.* 249 (2020) 118754. <https://doi.org/10.1016/j.conbuildmat.2020.118754>.
- [48] M. Balapour, W. Zhao, E.J. Garboczi, N.Y. Oo, S. Spatari, Y.G. Hsuan, P. Billen, Y. Farnam, Potential use of lightweight aggregate (LWA) produced from bottom coal ash for internal curing of concrete systems, *Cem. Concr. Compos.* 105 (2020) 103428. <https://doi.org/10.1016/j.cemconcomp.2019.103428>.
- [49] European Committee for Standardization, *EN 1097-6: Tests for mechanical and physical properties of aggregates. Part 6: Determination of particle density and water absorption.*, (2000).
- [50] C.R. Cheeseman, A. Makinde, S. Bethanis, Properties of lightweight aggregate produced by rapid sintering of incinerator bottom ash, *Resour. Conserv. Recycl.* 43 (2005) 147–162. <https://doi.org/10.1016/j.resconrec.2004.05.004>.
- [51] Y. Li, D. Wu, J. Zhang, L. Chang, D. Wu, Measurement and statistics of single pellet mechanical strength of differently shaped catalysts, *Powder Technol.* (2000) 176–184.
- [52] European Committee for Standardization, *EN 12457-4: Compliance test for leaching of granular waste materials and sludges. Part 4: One stage batch test at a liquid to solid ratio of 10 l/kg for materials with particle size below 10 mm (without or with size reduction).*, (2002).
- [53] European Committee for Standardization, *EN 196-1: Methods of testing cement. Part 1: Determination of strength.*, (2016).
- [54] American Society for Testing and Materials, *ASTM D5930: Standard Test Method for Thermal Conductivity of Plastics by Means of a Transient Line-Source Technique.*, (2001).

- [55] A. Maldonado-Alameda, A.M. Lacasta, J. Giro-Paloma, J.M. Chimenos, L. Haurie, J. Formosa, Magnesium phosphate cements formulated with low grade magnesium oxide incorporating phase change materials for thermal energy storage, *Constr. Build. Mater.* 155 (2017) 209–216. <https://doi.org/10.1016/j.conbuildmat.2017.07.227>.
- [56] A.I. Rat'Ko, A.I. Ivanets, A.I. Kulak, E.A. Morozov, I.O. Sakhar, Thermal decomposition of natural dolomite, *Inorg. Mater.* 47 (2011) 1372–1377. <https://doi.org/10.1134/S0020168511120156>.
- [57] N.H. Rodríguez, S.M. Ramírez, M.T.B. Varela, M. Guillem, J. Puig, E. Larrotcha, J. Flores, Re-use of drinking water treatment plant (DWTP) sludge : Characterization and technological behaviour of cement mortars with atomized sludge additions, *Cem. Concr. Res.* 40 (2010) 778–786. <https://doi.org/10.1016/j.cemconres.2009.11.012>.
- [58] A. Monem, M. Soltan, W. Kahl, F.A. El-raoof, B.A. El-kaliouby, M.A. Serry, N.A. Abdelkader, Lightweight aggregates from mixtures of granite wastes with clay, *J. Clean. Prod.* 117 (2016) 139–149. <https://doi.org/10.1016/j.jclepro.2016.01.017>.
- [59] J.A. Bogas, J. de Brito, J.M. Figueiredo, Mechanical characterization of concrete produced with recycled lightweight expanded clay aggregate concrete, *J. Clean. Prod.* 89 (2015) 187–195. <https://doi.org/10.1016/j.jclepro.2014.11.015>.
- [60] S.L. Sarkar, C. Satish, B. Leif, Interdependence of microstructure and strength of structural lightweight aggregate concrete, *Cem. Concr. Compos.* 14 (1992) 239–248. [https://doi.org/10.1016/0958-9465\(92\)90022-N](https://doi.org/10.1016/0958-9465(92)90022-N).
- [61] L. Chica, A. Alzate, Cellular concrete review: New trends for application in construction, *Constr. Build. Mater.* 200 (2019) 637–647. <https://doi.org/10.1016/j.conbuildmat.2018.12.136>.
- [62] K. Schumacher, N. Saßmannshausen, C. Pritzel, R. Trettin, Lightweight aggregate concrete with an open structure and a porous matrix with an improved ratio of compressive strength to dry density, *Constr. Build. Mater.* 264 (2020) 120167. <https://doi.org/10.1016/j.conbuildmat.2020.120167>.
- [63] American Society for Testing and Materials, ASTM C330 / C330M: Standard Specification for Lightweight Aggregates for Structural Concrete., (2009).
- [64] H.Z. Cui, T.Y. Lo, S.A. Memon, W. Xu, Effect of lightweight aggregates on the mechanical properties and brittleness of lightweight aggregate concrete, *Constr. Build. Mater.* 35 (2012) 149–158. <https://doi.org/10.1016/j.conbuildmat.2012.02.053>.
- [65] H. Weigler, S. Karl, Structural lightweight aggregate concrete with reduced density-lightweight aggregate foamed concrete, *Int. J. Cem. Compos. Light. Concr.* 2 (1980) 101–104. [https://doi.org/10.1016/0262-5075\(80\)90029-9](https://doi.org/10.1016/0262-5075(80)90029-9).
- [66] A. Sales, F.R. De Souza, W.N. Dos Santos, A.M. Zimer, F.D.C.R. Almeida, Lightweight composite concrete produced with water treatment sludge and sawdust: Thermal properties and potential application, *Constr. Build. Mater.* 24 (2010) 2446–2453. <https://doi.org/10.1016/j.conbuildmat.2010.06.012>.
- [67] P. Shafigh, H. Ghafari, H. Bin Mahmud, M.Z. Jumaat, A comparison study of the mechanical properties and drying shrinkage of oil palm shell and expanded clay lightweight aggregate concretes, *Mater. Des.* 60 (2014) 320–327. <https://doi.org/10.1016/j.matdes.2014.04.001>.

- [68] T.Y. Lo, H.Z. Cui, Spectrum analysis of the interfacial zone of lightweight aggregate concrete, *Mater. Lett.* 58 (2004) 3089–3095. <https://doi.org/10.1016/j.matlet.2004.05.071>.

